

RESEARCH

Open Access



Micromeria fruticosa and *Foeniculum vulgare* essential oils inhibit melanoma cell growth and migration by targeting MMP9 and NFκB signaling

Yousef Salama^{1*} and Nawaf Al-Maharik^{2*}

Abstract

Background Fennel (Fe), also known scientifically as *Foeniculum vulgare*, and *Micromeria fruticosa* are herbaceous plants endemic to the Mediterranean Region. The use of their essential oils for their health-promoting effects has been seen in Middle-Eastern societies, where they have been used as a type of traditional medicine. These oils have been used to treat a variety of diseases, including headaches, abdominal pains, skin and eye infections, colds, and wounds. This study looks at the chemical makeup of essential oils extracted from Palestine-grown fennel seeds and *Micromeria fruticosa* leaves. The anticancer properties of each essential oil, as well as the combined mixture of both oils, were evaluated against the melanoma cell line.

Results GC–MS was used to study the essential oils (EOs) from *Micromeria fruticosa* leaves and fennel seeds that were extracted by hydrodistillation. Analysis of *M. fruticosa* EO allowed the identification of 20 compounds, accounting for 97.73% of the EO's overall composition, with pulegone (81.77%), β-caryophyllene (2.95%), isomenthone (2.17%), piperitenone oxide (1.78%), and *p*-mentha-3-en-8-ol (1.38%) being the primary components. 24 phytochemicals were identified in the essential oil of fennel seeds, accounting for 100% of its composition, of which trans-anethole (93.69%), fenchone (3.93%), and sylvestrene (0.83%) were the major constituents. Although the EOs derived from *M. fruticosa* leaves and fennel seeds have shown potential for inhibiting the growth of several types of cancer, their impact on the proliferation and migration of melanoma cells has not been investigated. The results of our study demonstrate that the application of both oils, either separately or in combination (referred to as Mix-EO therapy), effectively suppressed the growth of melanoma cells in a manner that was dependent on the dosage. Furthermore, both treatments resulted in the upregulation of pro-apoptotic Bax and the downregulation of apoptosis-inhibiting Bcl2 expression in an in vitro setting. The anti-proliferative effects were confirmed using a murine melanoma model in vivo. Furthermore, both the individual EOs that were assessed and their combination (Mix-EO) exhibited inhibitory properties against the migration of melanoma cells. Both EOs and Mix-EO were found to decrease the intracellular levels of the transcription factor nuclear factor kappa B (NFκB) and one of its downstream targets, matrix metalloproteinase9 (MMP9), in melanoma and tumor-associated mesenchymal stem cells. Finally, we demonstrate for the first

*Correspondence:

Yousef Salama
yousef.ut@najah.edu
Nawaf Al-Maharik
n.maharik@najah.edu

Full list of author information is available at the end of the article



© The Author(s) 2023. **Open Access** This article is licensed under a Creative Commons Attribution 4.0 International License, which permits use, sharing, adaptation, distribution and reproduction in any medium or format, as long as you give appropriate credit to the original author(s) and the source, provide a link to the Creative Commons licence, and indicate if changes were made. The images or other third party material in this article are included in the article's Creative Commons licence, unless indicated otherwise in a credit line to the material. If material is not included in the article's Creative Commons licence and your intended use is not permitted by statutory regulation or exceeds the permitted use, you will need to obtain permission directly from the copyright holder. To view a copy of this licence, visit <http://creativecommons.org/licenses/by/4.0/>. The Creative Commons Public Domain Dedication waiver (<http://creativecommons.org/publicdomain/zero/1.0/>) applies to the data made available in this article, unless otherwise stated in a credit line to the data.

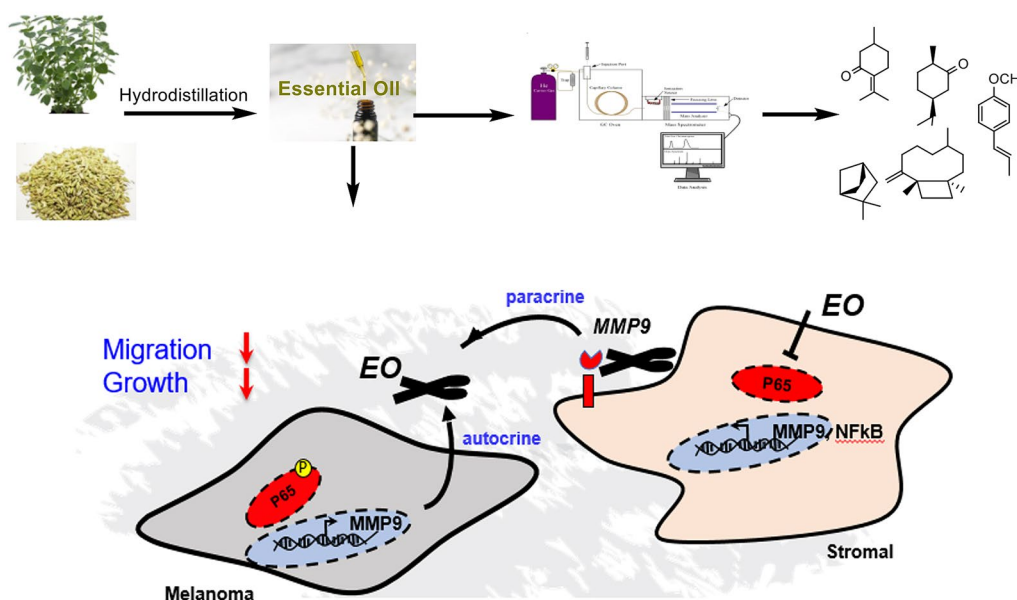
time that EOs from *M. fruticosa* leaves, fennel seeds, and their combination exert anti-cancer characteristics by inhibiting NFkB and MMP9 in melanoma (autocrine) and tumor-associated mesenchymal stem (paracrine) cells, thereby inducing melanoma cell apoptosis and preventing cell migration.

Conclusions The findings of our investigation indicate that the EOs derived from the fennel seeds and the *M. fruticosa* leaves encompass a diverse array of biologically active chemicals, which have robust anticancer effects. The results of this study hold promise for application in the advancement of innovative natural medications. Additional investigation is required to delve into the medicinal capacity of these essential oils in biological entities.

Keywords *Foeniculum vulgare*, *Micromeria fruticosa*, Essential oils, Anticancer, MMP9, NFkB, Melanoma

Graphical Abstract

M. fruticosa and *Foeniculum vulgare* essential oils Inhibit melanoma cell growth and migration by targeting MMP9 and NFkB signaling



Introduction

More than a decade ago, patients with metastatic melanoma had a 5-year survival rate of just 5%. The mainstream anti-melanoma therapy is a combination of drugs inhibiting BRAF and MEK kinase activity. In addition, new treatments such as immune checkpoint inhibitors or tumor-infiltrating lymphocytes are tested in patients with advanced melanoma [1]. Overall, these drugs extended the survival of some, but not all, patients [2]. Therefore, there is still an urgent need to identify effective treatments and elucidate the associated molecular mechanisms. Essential oils (EOs) are derived from fragrant plants [3], and their chemical components exhibit anti-tumor, antibacterial, anti-inflammatory, and diuretic

properties [4]. These properties are a result of intricate interactions among phenols, aldehydes, ketones, alcohols, esters, and ethers present in the EOs [5–8]. For instance, fennel, scientifically referred to as *Foeniculum vulgare*, is an herb that is native to the Mediterranean region and commonly used in many applications, such as cuisine (bread, pickles, and cheese), cosmetics, and pharmaceuticals. *Micromeria fruticosa*, a plant frequently encountered in the eastern Mediterranean region, synthesizes an EO consisting predominantly of the monoterpene pulegone, known for its anti-inflammatory characteristics [9].

Nuclear factor kappa B (NFkB) signaling is linked to inflammation [10]. NFkB regulates apoptosis, oncogenesis, and inflammation and is associated with melanoma

when overexpressed [11]. NFkB target genes include matrix metalloproteinases (MMPs), anti-apoptosis-associated *Bcl2*, and the pro-apoptotic gene *Bax*. These genes are linked to tumor growth. MMP-9 activation can promote the recruitment of niche cells such as cancer-associated fibroblasts, or MSC, endothelial cells, and inflammatory cells and contribute to melanoma progression [12, 13]. MMP9 activation in cutaneous melanoma is controlled by NFkB and associated with the BRAFV600E mutation [12, 13]. Upregulation of MMP9 has been indicated as a biomarker in melanoma. Tumor and tumor niche cells secrete MMP9 that hydrolyzes protein components of the extracellular matrix, thereby enhancing cell migration, proliferation, and invasion [14, 15].

Fennel EO (Fe-EO) shows anti-inflammatory and chemopreventive properties in patients with colon adenocarcinoma [16, 17]. Given the anti-inflammatory and tumor-suppressing properties demonstrated by Fe-EO and *M. fruticosa* (Thy-EO) in osteosarcoma cells [18], our objective was to investigate if these EOs may also inhibit the development of melanoma.

In this study, we analyzed the chemical compositions of fennel seed and *M. fruticosa* EOs and examined their individual and combined (Mix-EO) anti-cancer properties in vitro and in vivo. Tumor growth and migration were suppressed when Fe-EO or Thy-EO were given as monotherapy but completely blocked when combined. Mechanistically, Mix-EO downregulated NFkB and suppressed MMP9 expression in tumor and stromal cells. Restoration of MMP9 rendered melanoma cells resistant to the growth inhibitor effects of Mix-EO. MMP inhibitor treatment of non-melanoma/stroma cells suppressed MMP9 and NFkB expression in wild-type and MMP9-overexpressing cells and melanoma growth in wild type but not Mix-EO-cotreated cells. These data suggest that Mix-EO showed anti-melanoma properties by targeting NFkB and MMP9.

Experiment

Plant materials and essential oils extraction

M. fruticosa leaves and fennel seeds were gathered in August 2022 in Palestine's Jenin governorate (32° 27' 33'' N, 35°18' 03'' E, 161 m=528 feet above sea level). The plants were washed with distilled water before drying in the shade at room temperature and humidity (55 ± 4 RH). The dried materials were coarsely powdered, and the essential oils were extracted by hydro-distillation. The essential oils were dried with Na₂SO₄ and stored in sealed vials at 4 °C until further usage. The hydrodistillation of shade-dried plant leaves resulted in a pale yellow oil yield of 1.57%. The EO yield of fennel seeds was 4.5%.

Chromatographic analyses

Two replicates of each sample were analyzed using a Hewlett–Packard Model 5890 series II GC, equipped fused-silica capillary column (0.25 mm × 30 m, film thickness of 0.25 μm) and linked to Perkin Elmer Elite-5-MS (Perkin Elmer, USA). Helium was used at a flow rate of 1.1 mL/min.

Gas chromatography/mass spectrometry (GC/MS) analysis was performed as recently described in detail [19]. The injection port and detector temperatures were maintained at 250 °C. The oven temperature was programmed at 50 °C for 5 min followed by a ramp of 4.0 °C/min to 280 °C. 0.2 μL of the EO was injected in split mode with a splitting ratio of 1:50. The total running time was 62.50 min, and the solvent delay was from 0 to 4.0 min. The MS scan was covering a mass range of 50.00–300.00 m/z.

The identification of constituents was based on a comparison of the retention indices (RIs), calculated related to a standard mixture of n-alkanes (C₆–C₃₀) values and mass spectra with those obtained from authentic samples and/or the Nist, and on the interpretation of the EI-fragmentation of the molecules.

Chemicals and EOs

MTT (3-(4, 5)-dimethylthiazol (-z-y1)-3, 5-diphenyltetrazolium bromide) and fluorescein isothiocyanate (FITC)-phalloidin were purchased from Sigma (St. Louis, MO, USA). The Fe and Thy-EOs stock solution were isolated and dissolved in DMSO to a concentration of 500 μg/mL. We combined equal amount of each oil to achieve a final concentration of 500 μg/mL for the MIX-EO.

Cell lines

The murine melanoma B16F10 [CRL-6475; American Type Culture Collection (ATCC), Manassas, VA, USA], B16F1 (CRL-6323) and the mouse Embryonic Fibroblast-1 (MEF-1; ATCC CRL-2214) cell lines were maintained in high-glucose Dulbecco's Modified Eagle's Medium (DMEM with L-glutamine, phenol red (Fuji Film Wako, Osaka, Japan), 10% fetal bovine serum (FBS; G.E. Healthcare, Chicago, IL, USA), and 1% penicillin/streptomycin (P/S) (Nacalai Tesque, Kyoto, Japan). In addition, the murine MS-5 and human HS-5 stromal cells were cultured in Iscove's Modified Dulbecco's Medium (Wako, Japan) containing 10% FBS and 1% P/S. The human melanoma cell line SK-MEL-28 (ATCC HTB-72) and the human epidermoid carcinoma cell line A431 (ATCC CRL-1555) were expanded in Eagle's Minimum Essential Medium containing 10% FBS. Human umbilical vein endothelial cells (HUVECs) were cultured at 37 °C/5% CO₂ on 0.1% gelatin (Wako Pure Chemicals)-coated culture plates (Falcon) in endothelial growth medium-2

(EGM-2; Lonza; cc4176). The T17B cell line was cultured in DMEM, 10% FBS, and 1%P/S. B53 (kindly provided by Ko Okumura; Juntendo University School of Medicine, Japan), were cultured in RPMI-1640 medium containing 10% FBS and 1% P/S. The human embryo kidney HEK293 (CRL-1573) cell line was maintained in high-glucose Dulbecco's Modified Eagle's Medium (DMEM with L-glutamine, phenol red (Fuji Film Wako, Osaka, Japan), 10% fetal bovine serum (FBS; G.E. Healthcare, Chicago, IL, USA), and 1% penicillin/streptomycin (P/S) (Nacalai Tesque, Kyoto, Japan).

Small interfering ribonucleic acids (siRNA)-based gene knockdown

B16F10 or MS-5 cells (2×10^5 cells/well) were seeded in 6-well plates, kept overnight (16 h) before transfection using siRNA (Invitrogen (Thermo Fisher Scientific, Lafayette, CO, USA) to target mouse MMP9. Cells were transiently transfected using Lipofectamine RNAiMAX (Invitrogen) [20]. We quantified the transfection efficiency using qPCR of the target gene in Si-target gene and Si-ctrl transfected cells. The following siRNAs were utilized to target human MMP-9:

Si-MMP9-5'-ACCUCCACUAUGUGUCCACUAUA-3'.

Si-Ctrl, 5'-GCUCCACAGAGUAUACCUU-3'.

Quantitative reverse transcriptase-polymerase chain reaction (qPCR)

Total RNA and cDNA generation and qPCR methods are described in detail in [21]. Each qPCR experiment was performed in triplicate and independently repeated two times. The respective primers used are:

Forward; Reverse.

m-TIMP-1 5'-AGGTGGTCTCGTTGATTTCT-3';
5'-CTAAGGCCTGTAGCTGTGCC-3.

m-TIMP-2 5'-GACTTCATTGTGCCCTGGGA-3';
5'-CAGCCCATCTGGTACCTGTG-3.

m-TIMP-3 5'-CTTTGTGGAGAGGTGGGACC-3';
5'-CCCAGGTGGTAGCGTAATT-3.

m-MMP9 5'-AGACGACATAGACGGCATCC-3';
5'-TCGGCTGTGGTTCAGTTGT-3.

m-P65 5'-CCTCTGCTTCCAGGTGACAG-3';
5'-ATGTGAGAGGACAGGGTCA-3.

m-BAX 5'-AGGCCTCCTCTCTACTTCG-3';
5'-GTGAGGACTCCAGCCACAAA-3.

m-BCI-2 5'-CCACCTGTGGTCCATCTGAC-3';
5'-ATCTCTGCGAAGTCACGACG-3.

m-β-actin 5'-CTAAGGCCAACCGTGAAAAG-3';
5'-ACCAGAGGCATACAGGGACA-3.

h-TIMP-1 5'-CAAAGTGCAGAGTGGCACTC-3';
5'-GGGACTGGAAGCCCTTTTCA-3.

h-TIMP-2 5'-CTGTGACTTCATCGTGCCT-3';
5'-CAGCCCATCTGGTACCTGTG-3.

h-TIMP-3 5'-GGCCTTAAGCTGGAGGTCAA-3';
5'-ACAGCCCCGTGTACATCTTG-3.

h-MMP9 5'-GGACTCGGTCTTTGAGGAGC-3';
5'-CCTGTGTACACCCACACCTG-3.

h-β-actin 5'-AGACCTGTACGCCAACACAG-3';
5'-TTCTGCATCTGTCTGGCAAT-3.

h-P65 5'-CCAATGGCCTCCTTTCAGGA-3';
5'-CTGATCTGACTCAGCAGGGC-3.

h-BAX 5'-GCCGGAAGTATCAGAACCA-3';
5'-GTCTTGGATCCAGCCCAACA-3.

h-BCI-2 5'-CATGTGTGTGGAGAGCGTCAAC-3';
5'-CAGATAGGCACCCAGGGTGAT-3.

Human MMP9 cloning

We used the genomic DNeasy Extraction Kit (Qiagen, Germany) to isolate HUMAN MMP9 coding sequence from A549 lung cell line and cloned the sequence into the LV-EF-L3T4-IRES2-EGFP vector. The MMP9 cloning sequence was XhoI, 5-GGGCTCGAGATGAGCCTC TGGCAGCCC-3 and EcoRV, 5-CCCGATATCCTAGTC CTCAGGGCACTGCAG-3. The purified fragment was inserted into the XhoI and SmaI sites of the eukaryotic expression vector LV-EF-L3T4-IRES2-EGFP. In addition, cloned plasmids were sequenced by Sanger sequencing (An-Najah University, Palestine) and amplified in *E. coli* DH5α competent cells.

Lentivirus production for (MMP9 OE)

Vesicular stomatitis virus glycoprotein-pseudotyped lentivirus was prepared using a three-plasmid system as described previously [21, 22] using the LV-EF-L3T4-IRES2-EGFP (kindly provided by Dr. Trono's laboratory and modified by Dr. Tomoyuki Yamaguchi, IKAKEN) with or without gene of interest, pMDL, and vesicular stomatitis virus glycoprotein envelope plasmid VSV.G (Addgene #14886).

Western blot analysis

Sample preparation and protein transfer to PVDF membranes (Millipore, Immobilon) as described recently [21]. The membranes were probed with one of the following primary antibodies (all mouse IgG, 1 μg/ml) overnight at 4 °C: NFκB of mouse origin (Santa Cruz Biotech, sc-109), MMP9 (Santa Cruz Biotech, sc-6840) β-actin (Cell Signaling, #4967). In addition, membranes were stained with secondary antibody conjugated with horseradish peroxidase (Nichirei Biosciences INC, rabbit-HRP, or mouse-HRP) and developed with the ECL Plus detection system (Amersham Life Science, RPN2132) using image analyzer C-280 Azure (azure Biosystems).

Cell cultures with EOs

B16F10 or A431 cells (2×10^5 cells/well) were cultured in 6-well plates (TPP, Switzerland) and incubated overnight prior to the addition of DMSO (EO control), Thy-EO, Fe-EO, or Mix-EO at doses ranging from 5 to 50 $\mu\text{g}/\text{ml}$. EOs were used in the proliferation assays at a concentration of 25 $\mu\text{g}/\text{ml}$, unless specified otherwise. Viable cells were counted at 24 h using trypan blue dead-cell exclusion dye (cat. 207-17081; Fuji Film Wako). Cell proliferation was also estimated using the MTT assay kit (Sigma, St. Louis, MO, USA). In some experiments, B16F10 were seeded at a 5×10^4 cells/6-well concentration 16 h before the addition of rec. human MMP9 (100 ng/ml; Peprotech) in the presence/absence of Mix-EO (25 ng/ml).

MS-5 conditioned medium: for MMP9 knockdown and (MMP9 OE), MS-5 cells were seeded at a concentration of 5×10^5 cells/6-well for 16 h before transfection or infections, respectively. After 12 h, the transfection media was replaced with fresh media. Specific gene-targeting and control non-specific targeting siRNAs were obtained from Invitrogen (Thermo Fisher Scientific, Lafayette, CO). Cells were treated with or without the MMP inhibitor MMI270 (10 μM ; Novartis). Supernatants were collected after 24 h. The B16F10 culture medium was replaced with the MS-5 conditioned medium. 24 h later, B16F10 cell proliferation was determined.

Scratch assay

B16F10 cells were cultured in 6-well plates (2×10^5 cells/well in a 6-well plate) with DMEM complete medium containing indicated EO combinations at a concentration of 25 $\mu\text{g}/\text{ml}$ (Mix-EO were 12.5 $\mu\text{g}/\text{ml}$ of Fe-EO and 12.5 $\mu\text{g}/\text{ml}$ of Thy-EO). A scratch was performed vertically using a sterile yellow tip to scratch the 6-well plate perpendicular to its bottom when cells were sub-confluent, with two lines of similar width per well. After washing gently with PBS three times, DMEM complete medium was re-administered.

Murine B16F10 melanoma model

8–12-week-old male WT. C57BL/6 mice (Palestine) were housed under specific pathogen-free conditions. A subcutaneous murine melanoma model was employed: B16F10 cells were washed twice with PBS (90% viability). Then, cells were inoculated on d 0 ($5 \times 10^6/200 \mu\text{L}/\text{mouse}$, s.c.) into C57/BL6 mice. The in vivo treatment included: EO (30 mg/kg body weight) or carrier (DMSO/PBS) were injected intraperitoneally daily starting on day 0 after B16F10 tumor cell injection. We evaluated tumor growth daily. Mice that showed severe pain, with a weight loss > 20% compared to the initial body weight, or appeared moribund were euthanized. Removed tumors and adjacent conjunctive tissues were weight 12 days

after s.c. tumor cell injection. Blood plasma and tumor tissue samples were stored at -30°C until further usage.

Isolation of tumor-associated murine mesenchymal stem cells (MSCs)

Single-cell suspensions were prepared from extracted tumors, and tumor-associated MSCs were isolated using MagCollect™ Mouse Mesenchymal Stem Cell Isolation Kit; Catalog Number: MAGM212B from R&D system as instructed by the manufacturer. As a control, MSCs were isolated from the bone marrow of C57/BL6 mice that did not carry a tumor (WT).

MMP9 ELISA

Plasma samples were measured using a commercially available mouse-specific enzyme-linked immunosorbent assay (ELISA) kit for mouse MMP9 (R&D Systems, Minneapolis, MN, USA). Each sample was measured in duplicate.

Webserver timer

TIMER is a comprehensive web server, and resource for systematically analyzing the correlation between gene expression and immune infiltrates across diverse cancer types (<http://gepia2.cancer-pku.cn/#index>) [22].

Statistical analysis

All experiments were performed at least three times. Data are shown as the mean \pm standard error of the mean (SEM). Student's *t* test or ANOVA with Tukey HSD posthoc tests using R program were used for statistical analysis. *P* values < 0.05 were considered statistically significant.

Results and discussion

GC–MS analyses of essential oils

The output of EO of fennel in this study was 4.5%, with 25 components accounting for 99.97% of its total content (Table 1). According to prior research, production ranges from 1.3% to more than 6.4% depending on geographical origin and harvest period [16]. The composition of EO could be divided into two groups: oxygenated monoterpenes (98.66%) and monoterpene hydrocarbons (1.31%), with the primary constituents being trans-anethole (93.69%), fenchone (3.93%), sylvestrene (0.83%), and methyl chavicol (0.57%) (Table 1). Several earlier research on the variation of fennel EOs in different regions have all confirmed the existence of trans-anethole as a major component ranging from 35% to 84% [23]. Roby et al. [24] reported the identification of 15 compounds representing 95% of the oil, of which the major constituents

Table 1 Phytochemical composition of fennel (*Foeniculum vulgare*) seed EO collected from the Nablus region, Palestine

Compound	R.T	RI	Content%
α -Pinene	9.79	931	0.06
Camphene	10.51	947	0.01
Sabinene	11.56	970	0.01
β -Pinene	11.75	974	0.08
Myrcene	12.35	987	0.08
Phellandrene	13.04	1003	0.10
<i>p</i> -Cymene	13.84	1022	0.05
Sylvestrene	14.11	1028	0.83
1,8-Cineole	14.13	1030	0.01
cis-Ocimene	14.40	1035	0.10
trans-Ocimene	14.83	1045	0.00
γ -Terpinene	15.31	1056	0.09
Fenchone	16.71	1089	3.93
Allo-Ocimene	18.00	1126	0.01
Camphor	18.87	1144	0.11
Terpinen-4-ol	20.23	1178	0.01
Methyl chavicol	20.92	1196	0.57
Octanol acetate	21.34	1207	0.01
endo-Fenchyl acetate	21.60	1215	0.03
exo-Fenchyl acetate	22.10	1229	0.16
cis- <i>p</i> -Anethole	22.89	1251	0.02
<i>p</i> -Anisaldehyde	23.02	1254	0.00
trans-Anethole	24.43	1294	93.69
Germacrene D	30.50	1480	0.01
Total			99.98
Monoterpene hydrocarbons			1.31
Oxygenated monoterpenes			98.66
Sesquiterpene hydrocarbons			0.01
Oxygenated sesquiterpenes			0.00

RT Retention time, RI Retention index

were trans-anethole (56.4%), fenchone (8.26%), estragole (5.21%), methyl chavicol (5.2%), and limonene (4.2%). The chemical composition of EO derived from fennel seeds collected in Sichuan Province was investigated using gas chromatography–mass spectrometry (GC–MS) [25]. A total of 28 components were identified, with trans-anethole being the predominant compound, constituting 68.53% of the overall composition. The principal components of the composition identified were estragole, limonene, and fenchone, accounting for 10.42%, 6.24%, and 5.45% of the composition, respectively. Using gas chromatography with flame ionization detection and mass spectrometry (GC–FID–MS), the chemical composition of EOs in 56 samples of wild fennel seeds taken from diverse locations in Sicily was examined [26]. The investigation resulted in the identification of 78 distinct compounds, collectively constituting more than 98%

Table 2 Chemical components of *M. fruticosa* leaves's EO collected from the Genin region, Palestine

Compound	R.T	RI	Content%
α -Pinene	9.78	931	0.12
β -Pinene	11.73	974	0.33
Myrcene	12.32	987	0.11
Limonene	14.02	1026	0.86
<i>p</i> -Mentha-3,8-diene	15.81	1063	0.34
<i>p</i> -Mentha-3-en-8-ol	19.05	1149	1.38
Isomenthone	19.56	1162	2.17
trans-3-Pinanone	19.96	1172	1.27
α -Terpineol	20.80	1193	0.29
Verbenone	21.24	1205	0.77
ND	21.56	1214	1.01
Pulegone	22.46	1239	81.77
Piperitone	22.91	1251	0.16
trans-Anethole	24.05	1289	1.36
Piperitenone	25.83	1336	1.04
Piperitenone oxide	26.59	1358	1.78
β -Caryophellene	28.56	1418	2.95
α -Caryophellene	29.68	1454	0.18
Germacrene D	30.48	1480	0.74
Bicyclgermacrene	30.94	1495	0.29
Caryophyllene oxide	33.53	1582	1.09
Total identified			97.73
Monoterpene Hydrocarbons			1.76
Oxygenated monoterpenes			90.72
Sesquiterpene hydrocarbons			4.16
Oxygenated sesquiterpenes			1.09

of the EOs. Estragole was found to be the main component in 55 out of the EOs examined. Its amounts varied between 34% and 89%. However, the trans-anethole content showed significant heterogeneity, ranging from 0.1% to 36% across the samples analyzed. Fenchone, an oxygenated monoterpene frequently present in fennel oil, was detected in all samples, with concentrations ranging from 2% to 27%. All samples included monoterpene hydrocarbons, including α -pinene (1–21%), limonene (1–17%), and γ -terpinene (<1–4%). Shahat et al. investigated the chemical composition of EOs extracted from Egyptian wild and cultivated fennel aerial parts [27]. The EO of wild fennel contained twenty components, the most abundant of which was limonene (84.49%), followed by trans-anethole (6.22%), and α -pinene (2.03), with estragole accounting for only 0.05%. In EO derived from cultivated fennel, however, 21 chemicals were detected, with α -pinene (32.82%), estragole (15.33%), trans-anethole (14.84%), limonene (13.92%), and fenchone (5.91%) being the predominant ingredients [27].

Twenty components were detected in the EO from *M. fruticose* leaves, accounting for 97.73% of the total area (Table 2). Oxygenated monoterpenes account for 90.72% of the total, followed by sesquiterpene hydrocarbons (4.16%), monoterpene hydrocarbons (1.7%), and oxygenated sesquiterpenes (1.0%). Pulegone (81.77%), β -caryophellene (2.95%), isomenthone (2.1%), piperitenone oxide (1.78%), and trans-anethole (1.36%) were the major compounds (Table 2). The results of our study exhibited a degree of agreement with the previously published data on the chemical composition of the EO of *M. fruticose* leaves collected in Nablus, Palestine [28]. In that particular study, a total of 35 chemical constituents were identified, with pulegone being the predominant compound (58.7%), followed by neoisomenthole (8.7%), β -caryophellene (3.9%), and isomenthone (3.9%). Alqarni et al. [29] reported the identification of 33 components in fresh, shadow-dried and freeze-dried oil samples of *M. fruticose* collected from Hebron-Palestine, of which menthole (33.19–35.01%), menthone (17.47–20.40%) and pulegone (13.79–23.70%) were the major constituents. In addition, 61 compounds were identified from the EO extracted by hydrodistillation of *M. fruticosa* aerial parts growing wild in southern Italy, representing 91.3% of the oil, of which γ -terpinene (14.5%), β -caryophyllene (12.6%), *p*-cymene (8.9%), α -pinene (8.2%), and β -bisabolene (7.2%) were the major components [30].

Fe and Thy EO co-treatment induce cell apoptosis in melanoma cells

The chemical structures of pulegone and trans-anethole, the main components of Thy-EO and Fe-EO, and other major EO compounds are given in Fig. 1A. Reports indicate that anethole and pulegone exert anti-inflammatory effects, while anethole also has anti-tumor capabilities [31]. In addition, anethole suppresses NF κ B activation by I κ B α degradation [9].

Different concentrations of Fe-EO and Thy-EO were tested for their effects on cell proliferation in the highly metastatic murine B16F10 and human amelanotic A431 melanoma cell lines. As shown in Fig. 1B, Fe-EO and Thy-EO inhibited proliferation of B16F10 and A431 cells in a concentration-dependent manner after 24 h of treatment in vitro. On the other hand, control treatment (DMSO) did not influence cell proliferation (Fig. 1B). To capitalize on the putative anti-cancer properties and compound profile differences of both essential oils, Fe-EO and Thy-EO (Mix-EO) were introduced into the aforementioned melanoma cell lines. While Fe-EO or Thy-EO monotherapy at a concentration of 25 μ g/ml blocked B16F10 cell growth by ~25%, Mix-EO at the same concentration suppressed B16F10 or A431 cell growth by ~75% compared to carrier treatment (Fig. 1B, C). Tumor growth

was blocked entirely at a concentration of 50 μ g/ml given as single EOs and Mix-EO (Fig. 1B, C). Mix-EO addition to B16F10 cultures caused 50% cell death at a concentration between 5 and 25 μ g/ml, as determined using the MTT cell proliferation assay (Fig. 1D).

The concentrations producing 50% growth inhibition (IC₅₀) of Fe-EO on B16F10 and A431 cells were 30.9 and 32.1 μ g/ml, respectively, and those of Thy-EO were 31.6 and 33.3 μ g/ml, respectively (Table 3). The IC₅₀ of Mix-EO on B16F10 and A431 cells was 14.1 μ g/ml and 12.1 μ g/ml, respectively (Table 3). Myelotoxicity is a dose-limiting toxicity of anti-cancer drugs. Adding up to 25 μ g/ml of Mix-EO was not cytotoxic for peripheral blood mononuclear cells (PBMCs) (Fig. 1E). These data indicate that Mix-EO potentiated the anti-proliferative effects compared to the separate EOs given as monotherapy, enabling drug reduction and minimizing myelotoxicity.

Examination of the morphology of Mix-EO-treated B16F10 cells revealed apoptotic cells occurring in cultures treated with 25 μ g/ml after 24 h. Higher concentrations were necessary to induce apoptotic cell accumulation in cultures treated with Fe-EO and Thy-EO (not shown). Next, we tested the effect of the EOs on the expression of the pro-apoptotic gene Bax and the anti-apoptotic gene Bcl2. The transcript expression levels of Bax increased after Mix-EO treatment in cultured B16F10 and A431 cells (Fig. 1G, H). In contrast, the apoptosis-inhibiting Bcl2 gene was downregulated in Mix-EO-treated B16F10 and A431 cells (Fig. 1G, H), suggesting that Mix-EO-induced apoptosis in melanoma cells.

MMP9 reduction and impaired melanoma motility after Fe- and Thy-EO, and Mix-EO

Matrix metalloproteinases (MMPs), such as MMP-9, facilitate the breakdown of the extracellular matrix (ECM), hence promoting the spread of melanoma into the surrounding tissues [15]. We investigated the expression of MMP9 in both melanoma and non-melanoma cell lines due to the inhibitory effect of EOs on cell migration and the observed elevated levels of this protein in specific forms of melanoma. Based on the qPCR results, it was observed that murine B16F10 cells exhibited a greater level of MMP9 expression compared to B16F1 cells, which had a limited ability to metastasize. In addition, the malignant B cell line B53, mouse embryonic fibroblasts (MEF), and murine stromal fibroblastic MS-5 cells also showed lower MMP9 expression levels, as shown in Fig. 2A.

The levels of MMP9 were elevated in both human SKMEL28 melanoma and A431 cells. Figure 2B shows

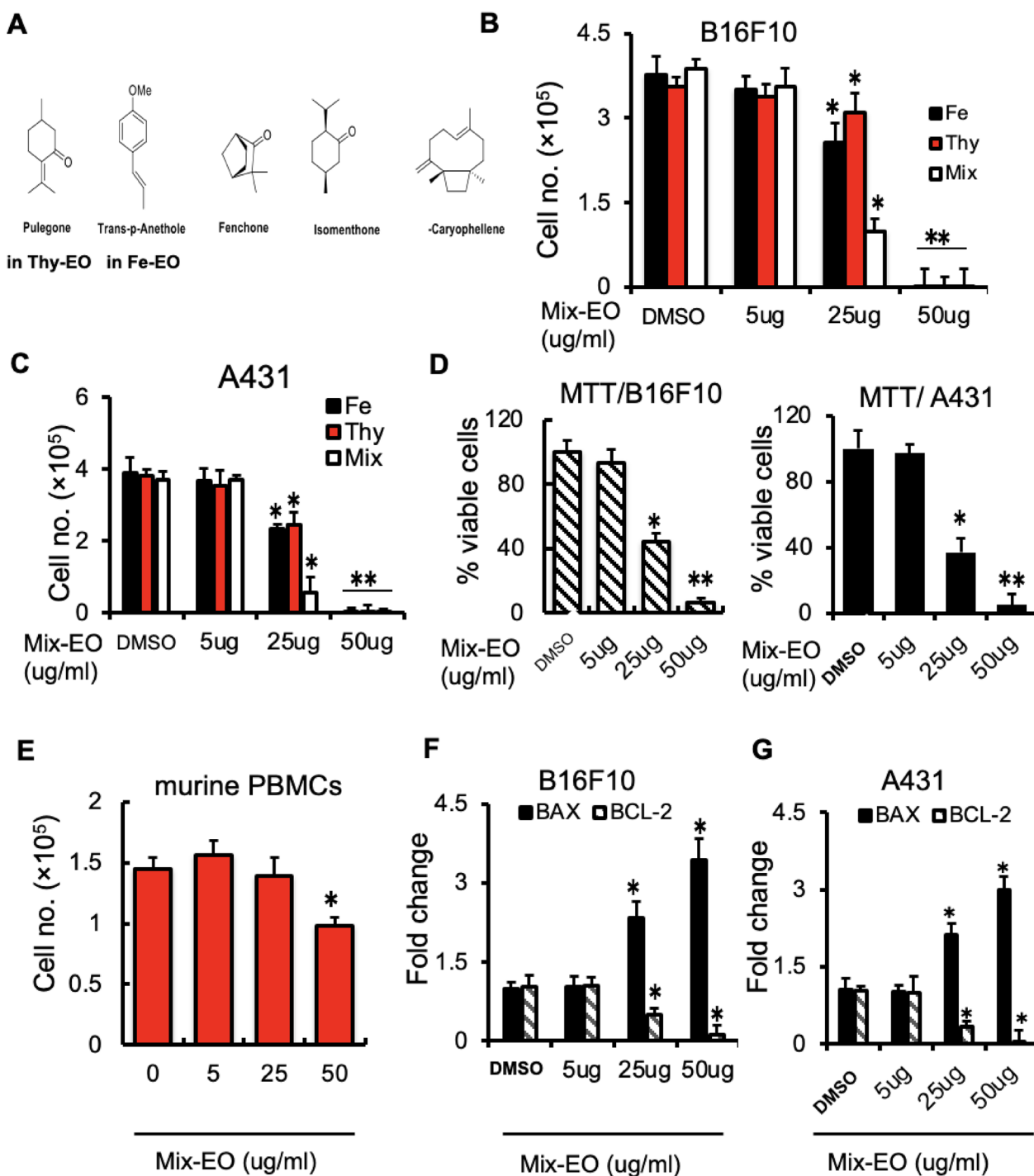


Fig. 1 Fennel (Fe) and *M. fruticosa* (Thy) EOs inhibit melanoma cell growth. **A** Molecular structures of the major components found in EOs of Fe and Thy. **B, C** Murine B16F10 (**B**) and A431 cells (**C**) were treated with indicated concentrations of Fe-OE, Thy-OE given as monotherapy or in combination (Mix-EO). Viable cells were counted using Trypan blue exclusion after 24 h ($n=6$ /group). **D** Cell viability of B16F10 and A431 cells exposed to indicated concentrations of Mix-EO was determined using an MTT assay ($n=6$ /group). **E** Cell viability of murine peripheral blood mononuclear cells (PBMCs) after treatment with Mix-EO at indicated concentrations ($n=6$ /group). **F, G** Fold changes in BAX and anti-apoptosis-related BCL2 gene expression in Mix-EO-treated and control B16F10 (**F**) and A431 (**G**) cells. Expressions were compared to carrier controls. Data are expressed as mean \pm SEM (unpaired Student's *t* test or one-way ANOVA $*p < .05$, $**p < .01$)

Table 3 Anti-cancer activity of EOs

Compounds IC50 values in (µg/mL)			
Cell line	Fe	Thy	Mix
B16F10	30.9	31.6	14.1
A431	32.1	33.3	12.1

IC₅₀ values on cancer cell lines (B16F10 and A431) after 24 h exposure to indicated EOs. Data are presented as half-maximal inhibitory concentration (IC₅₀) value from three independent experiments performed in triplication

that umbilical endothelial cells (HUVEC), human embryonic kidney 293 cells (HEK293), and stromal HS-5 cells all had lower amounts of MMP9. Through the utilization of an accessible human cancer database, we have ascertained that the levels of MMP9 were elevated in the tumor (T) of individuals diagnosed with skin cutaneous melanoma (SKCM) in comparison with the adjacent normal (N) skin tissues adjacent to the tumor (T) (Fig. 2C).

Subsequently, we analyzed the levels of MMP9 and its endogenous inhibitors, TIMP1-3, both prior to and following in vitro treatment with EO. EOs reduced the expression of MMP9 in A431 and B16F10 cells in a dose-dependent manner. However, the expression of TIMP1-3 was not affected by EOs (Fig. 2D, E; Additional file 1: Figure S1A, B). The study suggests that using Mix-EO treatment caused MMP9 expression to drop in melanoma cells. This may help explain how the essential oils studied could help fight cancer. Melanoma cells often have constitutively activated NF-κB [12, 32, 33]. The impact of single and combined EOs on the activation of NFκB was assessed due to its ability to regulate MMP9 expression. We found that Mix-EO-treated cells showed impaired P65 expression in B16F10 and A431 cells compared to control (Fig. 2F). Furthermore, Mix-EO and, to a certain degree, Thy-EO inhibited NFκB phosphorylation and activation, as assessed by Western blotting (Fig. 2G). To investigate the impact of Fe-EO, Thy-EO, and Mix-EO on melanoma cell motility, we conducted a wound scratch experiment due to the known association

between MMP9 and cell motility. Fe-, Thy-, and Mix-EO significantly decreased the migration of B16F10 cells (Fig. 2H, I) and A431 cells (Fig. 2J) by approximately 50% compared to the controls when administered at a dosage of 25 µg/ml. The data indicate that the Fe-EO, Thy-EO, and Mix-EO treatments inhibit cell migration.

Mix-EO suppressed in vivo melanoma growth and reduced intra-tumor MMP9

Next, we examined the effectiveness of Fe-, Thy-, and Mix-EO in controlling melanoma growth using the B16F10 subcutaneous melanoma model. For all EOs, the daily dosage was 30 mg/kg body weight. EO treatment started on day 0 after the initial tumor injection (Fig. 3A). Compared to controls (ctrl, carrier treatment), Fe-EO and Thy-EO treatment given intraperitoneally reduced tumor growth (Fig. 3A, B). Similar to our in vitro data, Fe- and Thy-EO monotherapy reduced tumor growth. However, tumor growth was blocked in Mix-EO-treated mice (Fig. 3A, B).

We confirmed a reduction of MMP9 expression in tumors of animals that had received Fe-EO, Thy-EO, and Mix-EO compared to control by qPCR (Fig. 3C), and a reduction of circulating MMP9 in peripheral blood as determined by ELISA (Fig. 3D). MMP9 expression was best suppressed after Mix-EO, not Fe- or Thy-EO mono treatment. Our data suggest that Mix-EO treatment abolished the tumor-mediated upregulation of MMP9.

Mix-EO blocks niche-derived MMP9

In melanoma, MMP-9 is expressed in tumor cells and stroma [34]. To test Mix-EO effects on MMP9 expression in tumor-associated mesenchymal stem cells (MSCs), we compared MMP9 expression of MSCs isolated from MSCs isolated from tumors of control and EO-treated mice to MSCs isolated from bone marrow (WT) by qPCR (Fig. 4A). All tested EOs completely suppressed MMP9 expression in MSCs. Because Mix-EO might induce apoptosis of niche cells, such as fibroblasts, we

(See figure on next page.)

Fig. 2 Combined treatment with Fe-EO and Thy-EO (Mix-EO) suppresses MMP9 expression and melanoma cell migration. (A and B) Murine B53, MEF, B16F1, B16F10, MS-5 (A) and human HEK293 HS-5, A431, SKMEL28, and HUVEC cells (B) were analyzed for MMP9 mRNA expression by qPCR ($n=3$ /cell line). Expression was compared to the expression in B53 (mouse) or HEK293 (human) cells. C Human MMP9 expression levels in tumor (T) and adjacent normal tissues (N) derived from SKCM patients. Data were retrieved from the TCGA database and analyzed by Tumor. D, E Fold change in MMP9 expression in B16F10 (D) and A431 (E) cells treated with indicated Mix-EO concentrations as determined by qPCR. Expression was compared to untreated controls. D, E Fold change in MMP9 expression in B16F10 (D) and A431 (E) cells treated with indicated concentrations of Mix-EO for 24 h as determined by qPCR. Expression was compared to the expression in control (DMSO)-treated cells. F Fold change in P65 expression in B16F10 and A431 cells treated with indicated concentrations of Mix-EO for 24 h ($n=6$ /group). G Representative immunoblots for p65, mouse MMP9, and b-actin (loading controls) using B16F10 cell lysates of indicated treatment groups. H–J Microscopic images 24 h after wound healing closure in B16F10 cultures treated with DMSO (control) or indicated EOs at indicated concentrations ($n=3$ /group). I Quantification of B16F10 cells that migrated in the scraped area indicated by thick lines per high power fields (HPF). A total of 5 × HPFs were counted. Data are expressed as mean ± SEM (unpaired Student's *t* test or one-way ANOVA * $p < .05$)

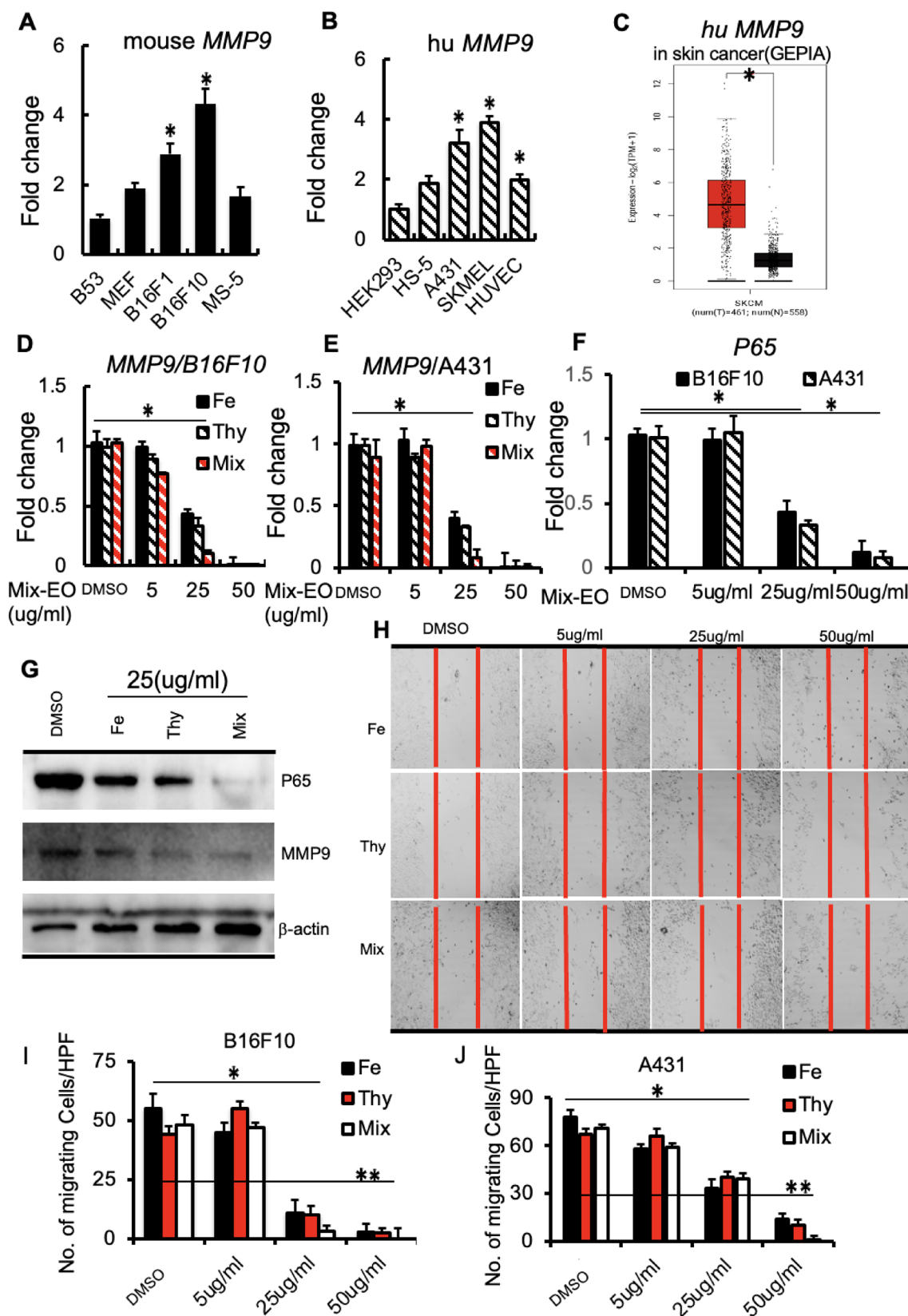


Fig. 2 (See legend on previous page.)

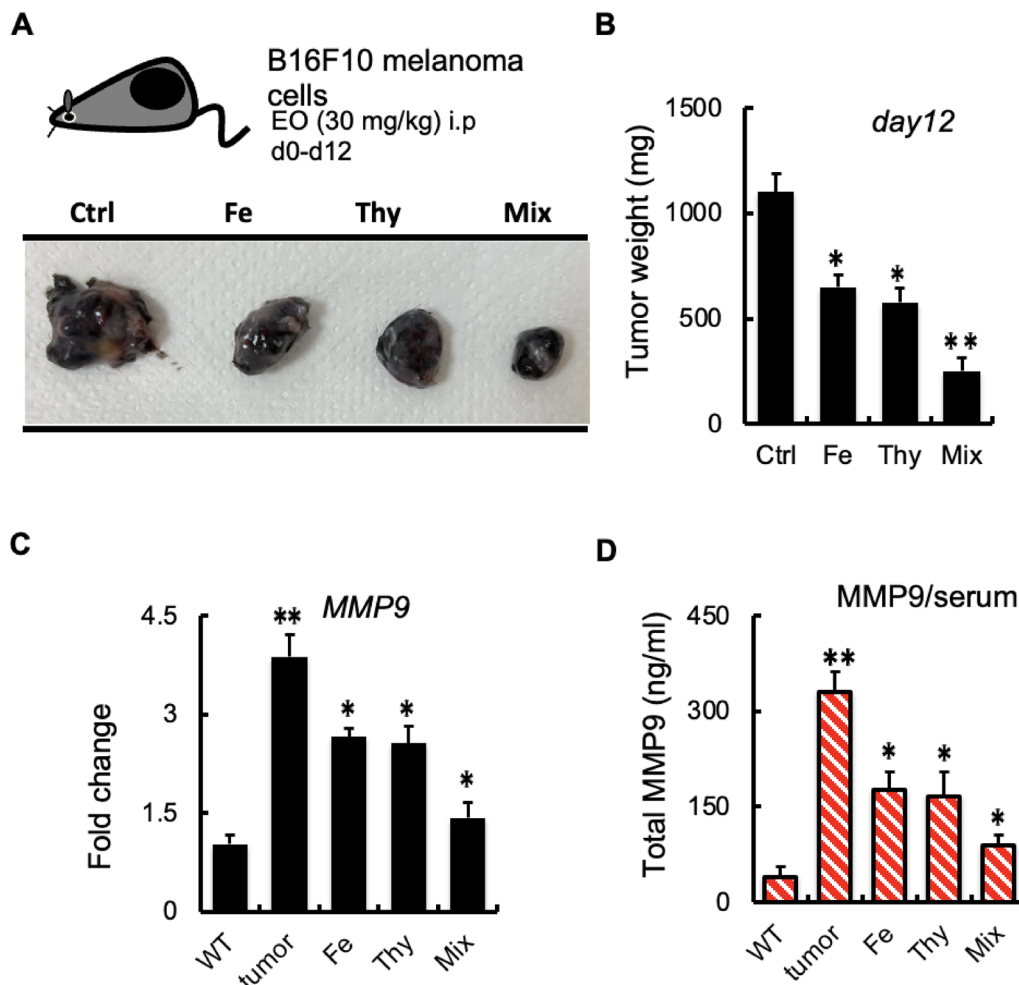


Fig. 3 Mix-EO treatment blocks melanoma growth in mice and suppresses systemic and tumor MMP9. **A–D** B16F10 cells were injected s.c. into the flank of C57/BL6 mice. Mice were treated with indicated dose combinations of EOs intraperitoneally (i.p.) daily starting from day 0. Twelve days after injection, microscopic tumor images were taken (**A**), and the tumor weight was measured (**B**; $n=6$ /group). **C** Collected tumors were analyzed for MMP9 expression by qPCR. Expression was compared to the expression in peripheral blood of non-tumor bearing mice (WT). **D** MMP9 plasma levels were determined on day 12 ($n=6$ /group). Data are expressed as mean \pm SEM (unpaired Student's t test or one-way ANOVA * $p < .05$, ** $p < .01$)

(See figure on next page.)

Fig. 4 Mix-EO treatment blocks tumor growth by targeting autocrine and paracrine MMP9 production. **A** Fold change in MMP9 expression in tumor-infiltrating mesenchymal stem cells (MSCs) isolated from mice treated with or without indicated EOs by qPCR. Expression was compared to bone-marrow-derived MSCs (WT) ($n=6$ /group). **B** Cell proliferation of B16F10 cells treated with/without rec. MMP9 in the presence/absence of 25 μ g/ml Mix-EO ($n=6$ /group). **C–G** Experimental outline to generate MS-5 conditioned medium for the treatment of B16F10 cells: collection of conditioned medium of MS-5 cells treated with carrier/DMSO (Ctrl) or Mix-EO (25 μ g/ml), MS-5 cells overexpressing hu MMP9WT (MMP9 OE) and cells, where mouse MMP9 had been gene-silenced (siMMP9) after 24 h ($n=6$ /group). **D** Fold change of MMP9 expression of MS-5 cells without (Ctrl) and with EO treatment (Mix-EO; 25 μ g/ml), after MMP9 OE, and gene silencing of MMP9 (si-MMP9). Expression was compared to the expression in ctrl cells ($n=6$ /group). **E–G** B16F10 cell growth was determined in cultures supplemented with indicated conditioned medium and cotreated with or without MMP inhibitor (MMPI) by Trypan blue 24 h later ($n=6$ /group). **F, G** Fold change in P65 (**F**) and MMP9 (**G**) expression in B16F10 cells treated with indicated MS-5 conditioned media in the presence or absence of MMPI ($n=6$ /group). Expression was compared to the expression in control cultures. Data are expressed as mean \pm SEM (unpaired Student's t test or One-way ANOVA * $p < .05$, ** $p < .01$). **H** Proposed mode of action of fennel (Fe-EO) and *M. fruticosa* (Thy-EO) derived EOs: Fe-EO and Thy-EO as monotherapy, but more prominent in combination (Mix-EO) inhibited NF κ B and MMP9 expression in tumor (autocrine action) and tumor stromal cells (paracrine action) suppressing tumor growth and migration. MMP9, matrix metalloproteinase-9; EO, essential oil; NF κ B, nuclear factor kappa B

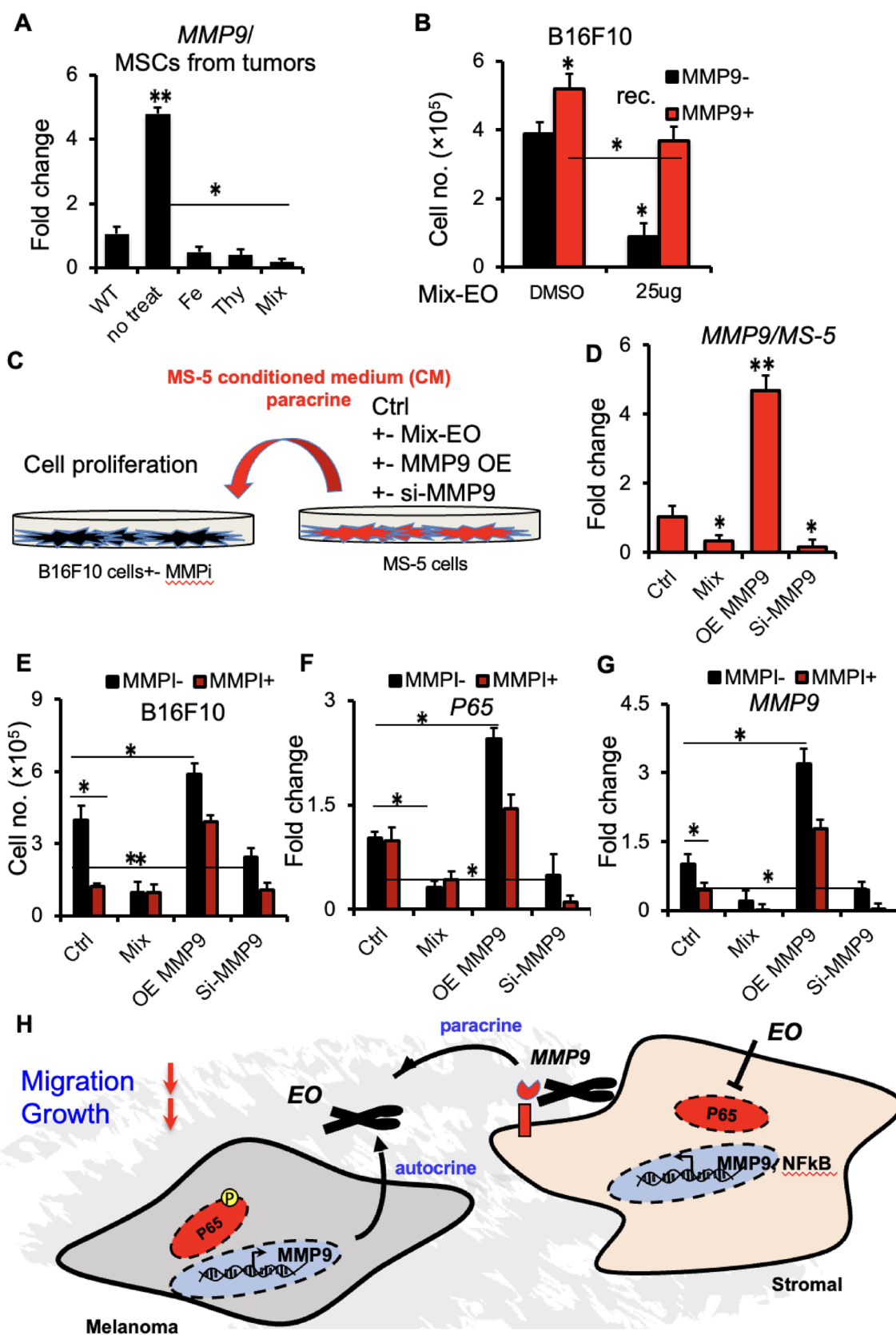


Fig. 4 (See legend on previous page.)

next tested cell proliferation of mouse embryonic fibroblasts (MEF) after Mix-OE treatment. At a dose of 50 $\mu\text{g}/\text{ml}$, Mix-OE did not inhibit the proliferation of MEF cells. This concentration had previously been determined to totally halt the growth of malignant melanoma cells (Additional file 1: Figure S1C). Addition of rec. MMP9 enhanced cell proliferation of B16F10 cells (Fig. 4B), an effect that the addition of Mix-OE could block. These data indicate that Mix-OE not only suppressed MMP9 transcription but also prevented MMP9 protein-mediated effects (Fig. 4B).

To test the effects of EOs on stromal cell-derived factors, such as MMP9, we established MS-5 cells, where MMP9 was gene-silenced (si-MMP9) or overexpressed using a lentivirus (MMP9 OE) and confirmed MMP9 expression in these cells by qPCR (Fig. 4D). Conditioned medium (CM) of (MMP9 OE) cells enhanced, while that of si-MMP9 cells inhibited cell proliferation. While adding an MMP inhibitor could suppress B16F10 proliferation in ctrl, (MMP9 OE), and siMMP9 cells, MMPI treatment could not further suppress Mix-OE-mediated cell proliferation (Fig. 4E), indicating that Mix-OE shares gene targets or pathways with the tested MMPI.

The addition of (MMP9 OE) CM augmented, while siMMP9 CM impaired tumor P65 and MMP9 expression (Fig. 4F, G). While the addition of an MMP inhibitor did not further reduce P65 and MMP9 expression in Mix-OE-treated cultures, suggesting that NF κ B signaling might be a target of Mix-OE. Overall, our data establish that EO from fennel and *M. fruticosa* when given in combination, synergistically suppress melanoma cell growth and migration while blocking NF κ B activation in tumor and stromal cells and the release of stromal cell tumor growth supporting factors, such as MMP9.

Trans-anethole has been shown to inhibit UV-induced melanogenesis [35]. The described anti-melanoma effects of the main compounds identified in Fe-EO and Thy-EO prompted us to examine the impact of Fe-EO and Thy-EO on melanoma. We show that Fe-EO and Thy-EO inhibit melanoma growth and migration in vitro. We identify MMP9 and the transcription factor NF κ B as targets of the EOs from fennel and *M. fruticosa*. The IC_{50} values of Mix-OE were 14.1 and 12.1 $\mu\text{g}/\text{ml}$ for the murine B16F10 and the human A431 melanoma cell lines, respectively. In contrast, a twofold higher concentration was necessary when Fe-EO or Thy-EO were given as monotherapy. The lower IC_{50} of Mix-EOs resulted in better tumor growth control than EO monotherapy in vivo. In addition, it allowed the use of a lower dosage of both EOs. At that low dosage, no myelotoxicity was observed. We propose that hepato-toxicity that had been

reported in mice treated with pulegone orally (>20mg/kg body weight/d) [36] might be avoided using Mix-OE. However, studies will be required to test this.

Tumor growth in mouse melanoma models was hindered by the suppression of MMP9 through the administration of synthetic MMP inhibitors or TIMP1, the endogenous inhibitor of MMP9 [37, 38]. We found that Mix-OE suppressed tumor and stromal cell-derived MMP9 and P65 expression, and contributed to melanoma growth and migration in vitro and in vivo. The decrease in MMP9 transcript levels caused by Mix-OE can be attributed to its impact on NF κ B signaling, as shown in Fig. 4H. In addition, Mix-OE suppressed tumor cell growth after the addition of rec. MMP9 or conditioned medium of MS-5 cells overexpressing MMP9. A possible explanation is that Mix-OE acts on proteins such as MMP9 or proteins such as cytokines released from MMP9-overexpressing MS-5/stromal cells. Further studies will be required to understand the underlying mechanism of Mix-OE on soluble factors, such as the MMP9 protein. Given the well-established role of MMP9 in tumor angiogenesis [39], further studies are required to determine the anti-angiogenic potential of Fe-EO, Thy-EO, and Mix-EO. MMP-9 has a dual role, in some cases, with anti-tumor activities. HPV16-related carcinomas are more aggressive in MMP9 null mice [40]. Bone-marrow-derived cell-derived MMP9 contributes to skin carcinogenesis [40].

The tested EOs mainly contain anethole and/or pulegone, which inhibit the phosphorylation of P65 in melanoma cells, indicating the suppression of NF κ B signaling. NF κ B regulates apoptosis, oncogenesis, and inflammation and is associated with melanoma when overexpressed [11]. Our data align with earlier reports demonstrating that pulegone inhibits NO production through suppressing iNOS, COX-2, NF κ B, and MAPKs signaling and up-regulating Nrf-2/HO-1 signaling in lipopolysaccharide-stimulated RAW264.7 cells [41]. Furthermore, trans-anethole exerts protective effects on lipopolysaccharide-induced acute jejunal inflammation of broilers via repressing the NF κ B signaling pathway [42]. In addition, reports indicate that anethole can inhibit TNF-induced NF κ B activation by suppressing I κ B α phosphorylation and NF κ B reporter gene expression induced by TRAF2 and NF κ B-inducing kinase. Furthermore, Anethole inhibited the nuclear localization of NF κ B protein PC-3 cells [43]. Given the observed NF κ B suppression, it is probable that the bioactive EOs also inhibit the recruitment of inflammatory cells that support tumors and their proteolytic activities. In addition, further research will be needed to identify the genes responsible for the combined benefits and synergistic effects of both EOs.

Conclusions

Treatment options for melanoma are limited. Altogether, our results support that EOs from fennel and *M. fruticosa* suppressed melanoma growth and migration and suppressed NF κ B signaling and MMP9 expression in tumor or tumor niche cells (Fig. 4H). A recent study proposed that melanoma cells overexpressing NF κ B are three times more likely to respond to treatment with checkpoint inhibitors and immunotherapy. It will be interesting to investigate if adding EOs to conventional chemotherapeutic agents, checkpoint inhibitors, or immunotherapy approaches will improve anti-melanoma properties.

Supplementary Information

The online version contains supplementary material available at <https://doi.org/10.1186/s40538-023-00522-4>.

Additional file 1: Figure S1. TIMP expression and MEF proliferation after Mix-EO treatment. **A, B** Fold change in Tissue inhibitors of metalloproteinase 1–3 expression in B16F10 **A** and A431 **B** cells after treatment with Mix-EO of B16F10 cells. Expression is compared to the expression in untreated controls ($n=6$ /group). **C** Murine embryonic fibroblasts (MEFs) were treated with indicated concentrations of Mix-EO. Viable cells were counted 24 h later by Trypan blue exclusion assay ($n=6$ /group). Data are expressed as mean \pm SEM (unpaired Student's t test or one-way ANOVA * $p < .05$).

Author contributions

Study concept and design (YS, NA); data acquisition (YS); analysis and interpretation of data (YS, NA); drafting of the manuscript (YS, NA); critical revision of the manuscript (YS, NA); obtained funding (YS, NA).

Funding

This work was supported partly by grants from An-Najah National University, Higher Council for innovation and Excellence/Palestine (Y.S.), Sukhtian Group/Palestine (Y.S.)

Availability of data and materials

Not applicable.

Declarations

Ethics approval and consent to participate

The study was conducted according to the guidelines of the Declaration of Helsinki. Animal study and euthanasia were carried out following the recommendations in the Guide for the Care and Use of Laboratory Animals of the National Institutes of Health. The protocol was approved by the Committee on the Ethics of Animal Experiments of the An Najah University (Ref: H.Sp. 2023/12).

Informed consent

Not applicable.

Competing interests

No competing interest exist.

Author details

¹An-Najah Center for Cancer and Stem Cell Research, Faculty of Medicine and Health Sciences, An-Najah National University, P.O. Box 7, Nablus 00970, Palestine. ²Department of Chemistry, Faculty of Sciences, An-Najah National University, P.O. Box. 7, Nablus 00970, Palestine.

Received: 21 October 2023 Accepted: 13 December 2023

Published online: 04 January 2024

References

- Falzone L, Salomone S, Libra M. Evolution of cancer pharmacological treatments at the turn of the third millennium. *Front Pharmacol.* 2018. <https://doi.org/10.3389/fphar.2018.01300>.
- Rohaan MW, Borch TH, van den Berg JH, Met Ö, Kessels R, Geukes Foppen MH, Stoltenborg Granhøj J, Nuijen B, Nijenhuis C, Jedema I, et al. Tumor-infiltrating lymphocyte therapy or ipilimumab in advanced melanoma. *N Engl J Med.* 2022;387:2113–25. <https://doi.org/10.1056/NEJMoa2210233>.
- Sharifi-Rad J, Sureda A, Tenore GC, Daglia M, Sharifi-Rad M, Valussi M, Tun-dis R, Sharifi-Rad M, Loizzo MR, Ademiluyi AO, et al. Biological activities of essential oils: from plant chemoeology to traditional healing systems. *Molecules.* 2017. <https://doi.org/10.3390/molecules22010070>.
- Cimino C, Maurel OM, Musumeci T, Bonaccorso A, Drago F, Souto EM, Pignatello R, Carbone C. Essential oils: pharmaceutical applications and encapsulation strategies into lipid-based delivery systems. *Pharmaceutics.* 2021. <https://doi.org/10.3390/pharmaceutics13030327>.
- Russo R, Corasaniti MT, Bagetta G, Morrone LA. Exploitation of cytotoxicity of some essential oils for translation in cancer therapy. *Evid Based Complement Alternat Med.* 2015;2015: 397821. <https://doi.org/10.1155/2015/397821>.
- Freires IA, Denny C, Benso B, de Alencar SM, Rosalen PL. Antibacterial activity of essential oils and their isolated constituents against cariogenic bacteria: a systematic review. *Molecules.* 2015;20:7329–58. <https://doi.org/10.3390/molecules20047329>.
- Bayala B, Bassole IH, Scifo R, Gnoula C, Morel L, Lobaccaro JM, Simpore J. Anticancer activity of essential oils and their chemical components - a review. *Am J Cancer Res.* 2014;4:591–607.
- Bakkali F, Averbeck S, Averbeck D, Idaomar M. Biological effects of essential oils: a review. *Food Chem Toxicol.* 2008;46:446–75. <https://doi.org/10.1016/j.fct.2007.09.106>.
- Chainy GBN, Manna SK, Chaturvedi MM, Aggarwal BB. Anethole blocks both early and late cellular responses transduced by tumor necrosis factor: effect on NF- κ B, AP-1, JNK. *Oncogene.* 2000;19:2943–50. <https://doi.org/10.1038/sj.onc.1203614>.
- Taniguchi K, Karin M. NF- κ B, inflammation, immunity and cancer: coming of age. *Nat Rev Immunol.* 2018;18:309–24. <https://doi.org/10.1038/nri.2017.142>.
- Pikarsky E, Ben-Neriah Y. NF- κ B inhibition: a double-edged sword in cancer? *Eur J Cancer.* 2006;42:779–84. <https://doi.org/10.1016/j.ejca.2006.01.011>.
- Guarneri C, Bevelacqua V, Polesel J, Falzone L, Cannavò PS, Spandidos DA, Malaponte G, Libra M. NF- κ B inhibition is associated with OPN/MMP-9 downregulation in cutaneous melanoma. *Oncol Rep.* 2017;37:737–46. <https://doi.org/10.3892/or.2017.5362>.
- Wu HT, Sie SS, Kuan TC, Lin CS. Identifying the regulative role of NF- κ B binding sites within promoter region of human matrix metalloproteinase 9 (mmp-9) by TNF- α induction. *Appl Biochem Biotechnol.* 2013;169:438–49. <https://doi.org/10.1007/s12010-012-9958-3>.
- Mehner C, Hockla A, Miller E, Ran S, Radisky DC, Radisky ES. Tumor cell-produced matrix metalloproteinase 9 (MMP-9) drives malignant progression and metastasis of basal-like triple negative breast cancer. *Oncotarget.* 2014;5:2736–49. <https://doi.org/10.18632/oncotarget.1932>.
- Napoli S, Scuderi C, Gattuso G, Di Bella V, Candido S, Basile MS, Libra M, Falzone L. Functional roles of matrix metalloproteinases and their inhibitors in melanoma. *Cells.* 2020. <https://doi.org/10.3390/cells9051151>.
- Salami M, Rahimmalek M, Ehtemam MH, Szumny A, Fabian S, Matkowski A. Essential oil composition, antimicrobial activity and anatomical characteristics of *Foeniculum vulgare* mill. Fruits from different regions of Iran. *J Essent Oil Bear Plants.* 2016;19:1614–26. <https://doi.org/10.1080/0972060X.2015.1117951>.
- Reddy BS, Rao CV, Rivenson A, Kelloff G. Chemoprevention of colon carcinogenesis by organosulfur compounds. *Can Res.* 1993;53:3493–8.

18. Peng L, Liu A, Shen Y, Xu HZ, Yang SZ, Ying XZ, Liao W, Liu HX, Lin ZQ, Chen QY, et al. Antitumor and anti-angiogenesis effects of thymoquinone on osteosarcoma through the NF- κ B pathway. *Oncol Rep.* 2013;29:571–8. <https://doi.org/10.3892/or.2012.2165>.
19. Al-Maharik N, Jaradat N, Al-Hajj N, Jaber S. *Myrtus communis* L.: essential oil chemical composition, total phenols and flavonoids contents, antimicrobial, antioxidant, anticancer, and α -amylase inhibitory activity. *Chem Biol Technol Agric.* 2023. <https://doi.org/10.1186/s40538-023-00417-4>.
20. Salama Y, Jaradat N, Hattori K, Heissig B. *Aloysia citrodora* essential oil inhibits melanoma cell growth and migration by targeting HB-EGF-EGFR signaling. *Int J Mol Sci.* 2021. <https://doi.org/10.3390/ijms22158151>.
21. Salama Y, Takahashi S, Tsuda Y, Okada Y, Hattori K, Heissig B. Y02 induces melanoma cell apoptosis through p53-mediated LRP1 downregulation. *Cancers.* 2023. <https://doi.org/10.3390/cancers15010288>.
22. Li T, Fan J, Wang B, Traugh N, Chen Q, Liu JS, Li B, Liu XS. TIMER: a web server for comprehensive analysis of tumor-infiltrating immune cells. *Can Res.* 2017;77:e108–10. <https://doi.org/10.1158/0008-5472.CAN-17-0307>.
23. Rahimmalek M, Sabzalian M, Ghasemi PA. Variability of essential oil content and composition of different Iranian fennel (*Foeniculum vulgare* Mill.) accessions in relation to some morphological and climatic factors. *J Agr Sci Tech.* 2014;16:1365–74.
24. Roby MHH, Sarhan MA, Selim KA-H, Khalel KI. Antioxidant and antimicrobial activities of essential oil and extracts of fennel (*Foeniculum vulgare* L.) and chamomile (*Matricaria chamomilla* L.). *Ind Crops Prod.* 2013;44:437–45. <https://doi.org/10.1016/j.indcrop.2012.10.012>.
25. Diao W-R, Hu Q-P, Zhang H, Xu J-G. Chemical composition, antibacterial activity and mechanism of action of essential oil from seeds of fennel (*Foeniculum vulgare* Mill.). *Food Control.* 2014;35:109–16. <https://doi.org/10.1016/j.foodcont.2013.06.056>.
26. Napoli EM, Curcuruto G, Ruberto G. Screening the essential oil composition of wild Sicilian fennel. *Biochem Syst Ecol.* 2010;38:213–23. <https://doi.org/10.1016/j.bse.2010.01.009>.
27. Shahat AA, Hammouda FM, Shams KA, Saleh MA. Comparative chemical analysis of the essential oil of wild and cultivated fennel (*Foeniculum vulgare* Mill.). *J Essent Oil Bear Plants.* 2012;15:314–9. <https://doi.org/10.1080/0972060X.2012.10644053>.
28. Shehab NG, Abu-Gharbieh E. Constituents and biological activity of the essential oil and the aqueous extract of *Micromeria fruticosa* (L.) Druce subsp. *serpyllifolia*. *Pak J Pharm Sci.* 2012;25:687–92.
29. Alqarni MH, Salkini AA, Abujheisha KY, Daghar MF, Al-khuraif FA, Abdel-Kader MS. Qualitative, quantitative and antimicrobial activity variations of the essential oils isolated from thymus vulgaris and *Micromeria fruticosa* samples subjected to different drying conditions. *Arab J Sci Eng.* 2022;47:6861–7. <https://doi.org/10.1007/s13369-021-06469-8>.
30. Formisano C, Mignola E, Rigano D, Senatore F, Bellone G, Bruno M, Rosselli S. Chemical composition and antimicrobial activity of the essential oil from aerial parts of *Micromeria fruticulosa* (Bertol.) Grande (Lamiaceae) growing wild in Southern Italy. *Flavour Fragr J.* 2007;22:289–92. <https://doi.org/10.1002/ffj.1795>.
31. Yang Q, Luo J, Lv H, Wen T, Shi B, Liu X, Zeng N. Pulegone inhibits inflammation via suppression of NLRP3 inflammasome and reducing cytokine production in mice. *Immunopharmacol Immunotoxicol.* 2019;41:420–7. <https://doi.org/10.1080/08923973.2019.1588292>.
32. Yang J, Richmond A. Constitutive I κ B kinase activity correlates with nuclear factor-kappaB activation in human melanoma cells. *Can Res.* 2001;61:4901–9.
33. Huang S, DeGuzman A, Bucana CD, Fidler IJ. Nuclear factor-kappaB activity correlates with growth, angiogenesis, and metastasis of human melanoma cells in nude mice. *Clin Cancer Res.* 2000;6:2573–81.
34. Kurschat P, Wickenhauser C, Groth W, Krieg T, Mauch C. Identification of activated matrix metalloproteinase-2 (MMP-2) as the main gelatinolytic enzyme in malignant melanoma by in situ zymography. *J Pathol.* 2002;197:179–87. <https://doi.org/10.1002/path.1080>.
35. Nam JH, Lee D-U. Foeniculum vulgare extract and its constituent, trans-anethole, inhibit UV-induced melanogenesis via ORAI1 channel inhibition. *J Dermatol Sci.* 2016;84:305–13. <https://doi.org/10.1016/j.jdermsci.2016.09.017>.
36. Thorup I, Würtzen G, Carstensen J, Olsen P. Short term toxicity study in rats dosed with pulegone and menthol. *Toxicol Lett.* 1983;19:207–10. [https://doi.org/10.1016/0378-4274\(83\)90120-0](https://doi.org/10.1016/0378-4274(83)90120-0).
37. Oku T, Ata N, Yonezawa K, Tokai H, Fujii H, Shinagawa A, Ohuchi E, Saiki I. Antimetastatic and antitumor effect of a recombinant human tissue inhibitor of metalloproteinases-2 in murine melanoma models. *Biol Pharm Bull.* 1997;20:843–9. <https://doi.org/10.1248/bpb.20.843>.
38. Khokha R. Suppression of the tumorigenic and metastatic abilities of murine B16–F10 melanoma cells in vivo by the overexpression of the tissue inhibitor of the metalloproteinases-1. *J Natl Cancer Inst.* 1994;86:299–304. <https://doi.org/10.1093/jnci/86.4.299>.
39. Heissig B, Hattori K, Friedrich M, Rafii S, Werb Z. Angiogenesis: vascular remodeling of the extracellular matrix involves metalloproteinases. *Curr Opin Hematol.* 2003;10:136–41.
40. Coussens LM, Tinkle CL, Hanahan D, Werb Z. MMP-9 supplied by bone marrow-derived cells contributes to skin carcinogenesis. *Cell.* 2000;103:481–90.
41. Roy A, Park H-J, Abdul QA, Jung HA, Choi JS. Pulegone Exhibits Anti-inflammatory Activities through the Regulation of NF- κ B and Nrf-2 Signaling Pathways in LPS-stimulated RAW 264.7 cells. *Nat Prod Sci.* 2018;24:28–35. <https://doi.org/10.20307/nps.2018.24.1.28>.
42. Tong Y, Yu C, Chen S, Zhang X, Yang Z, Wang T. Trans-anethole exerts protective effects on lipopolysaccharide-induced acute jejunal inflammation of broilers via repressing NF- κ B signaling pathway. *Poult Sci.* 2023;102:102397. <https://doi.org/10.1016/j.psj.2022.102397>.
43. Elkady A. Anethole inhibits the proliferation of human prostate cancer cells via induction of cell cycle arrest and apoptosis. *Anti-cancer Agents Med Chem.* 2017. <https://doi.org/10.2174/1871520617666170725165717>.

Publisher's Note

Springer Nature remains neutral with regard to jurisdictional claims in published maps and institutional affiliations.

Submit your manuscript to a SpringerOpen® journal and benefit from:

- Convenient online submission
- Rigorous peer review
- Open access: articles freely available online
- High visibility within the field
- Retaining the copyright to your article

Submit your next manuscript at ► [springeropen.com](https://www.springeropen.com)